

HIGH REYNOLDS NUMBER FLAT PLATE TURBULENT BOUNDARY LAYER EXPERIMENTS USING A HOT-WIRE RAKE SYNCHRONIZED WITH STEREO PIV

Joël Delville, Carine Fourment

Laboratoire d'Etudes Aérodynamiques, UMR CNRS 6609
47 route de l'Aérodrome, F-86036 Poitiers Cedex, France
joel.delville@lea.univ-poitiers.fr, carine.fourment@lea.univ-poitiers.fr

Murat Tutkun, Peter B. V. Johansson, William K. George

Turbulence Research Laboratory, Department of Applied Mechanics
Chalmers University of Technology, SE-41296 Gothenburg, Sweden
murat.tutkun@chalmers.se, peter.johansson@chalmers.se, wkgeorge@chalmers.se

Jim Kostas*, Sebastien Coudert, Jean-Marc Foucaut, Michel Stanislas

Laboratoire de Mécanique de Lille, UMR CNRS 8107
Bv Paul Langevin, Cité Scientifique F-59655 Villeneuve d'Ascq, France
dimitrios.kostas@univ-lille1.fr, sebastien.coudert@univ-lille1.fr, jean-marc.foucaut@ec-lille.fr,
michel.stanislas@ec-lille.fr

ABSTRACT

High Reynolds numbers zero pressure gradient flat plate turbulent boundary layer experiments have been carried out in the large wind tunnel of Laboratoire de Mécanique de Lille using synchronized PIV systems and a hot-wire rake of 143 single probes. The experiments were performed within the WALLTURB research project to create new data on wall turbulence at large Reynolds numbers. Tested Reynolds numbers based on the momentum thickness were 19100 and 9800. Experimental details and initial results are presented in the paper.

INTRODUCTION

The purpose of this paper is to report on the experimental setup details and some of the initial results of the zero pressure gradient high Reynolds number flat plate turbulent boundary layer experiments performed within the WALLTURB research program. The main aim of the experiment was to generate new data on high Reynolds number wall turbulence using the latest and the most advanced measurement techniques.

A great deal of understanding about turbulent boundary layers has been gained in the past few decades by means of experiments and numerical simulations. Unfortunately, most of the experiments carried out over this period were at low to moderate Reynolds numbers due to the restrictions imposed by the resolvable scales. The smallest scale that can be resolved in air is approximately $10\ \mu\text{m}$ and the smallest scale of the flow is the viscous length scale, ν/u_τ . Thus resolvable high Reynolds number flows are achievable only by increasing the boundary layer thickness while keeping the velocity relatively low. A large wind tunnel with 21.6 m long test section was built by Laboratoire de Mécanique de Lille (LML) in 1993 to be able to create high Reynolds number turbulent boundary layer flows with adequate spatial reso-

lution. A Reynolds number based on momentum thickness, Re_θ , of 20000 can be reached in the LML wind tunnel at 10 m/s wind tunnel freestream velocity while the boundary layer thickness is approximately 30 cm.

There has been significant development of measurement techniques in turbulence over the last decade. Much effort has been devoted to enabling Particle Image Velocimetry (PIV) to measure turbulent fluctuations with a high spatial resolution at a good accuracy (Foucaut et al. 2004). High sensitivity digital recording equipment with high signal-to-noise ratio together with rather sophisticated processing algorithms have made this non-intrusive technique a unique tool to obtain spatial information about the turbulent field.

There has also been advancements in the use of hot-wire anemometry measurement technique by construction of hot-wire rakes (HWR) of many probes (c.f., Delville et al., 1999, and Citriniti and George, 2000). This made the extraction of both spatial and temporal information on the turbulent flow possible.

Although PIV is a powerful technique to extract the spatial information from turbulent fields, temporal resolution is still limited. Hot-wire anemometry remains, however, an accurate and simple way of getting temporal dynamics of the flow at smaller scales with very high sampling frequencies. In this experiment, PIV and hot-wire anemometry were used together as complementary techniques to obtain both the spatial and temporal dynamics of the flow.

Two high Reynolds number flat plate experiments were carried out in the LML large wind tunnel using synchronized PIV systems and HWR of 143 single probes. Reynolds numbers of $Re_\theta = 9800$ and 19100 were tested at freestream velocities of 5 m/s and 10 m/s, respectively. The boundary layer thickness at the measurement location was about 30 cm. The experiments were performed jointly by the Laboratoire de Mécanique de Lille, Chalmers University of Technology and Laboratoire d'Etudes Aérodynamiques (LEA).

*Now at Department of Mechanical Engineering, Monash University, AU-3800 Victoria, Australia

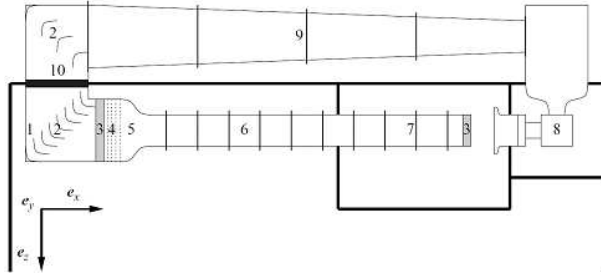


Figure 1: Schematic of the LML wind tunnel: 1, plenum chamber; 2, guide vanes; 3, honeycomb; 4, grids; 5, contraction; 6, turbulent boundary layer developing zone; 7, testing zone of wind tunnel; 8, fan and motor; 9, return duct; 10, heat exchanger (airwater).

EXPERIMENTAL SETUP

Wind Tunnel

Dimensions of the LML wind tunnel test section are 21.6 m in length, 1 m in height and 2 m in width. The maximum freestream velocity of the tunnel is about 10.5 m/s and constant velocity can be obtained with a precision better than 1%. Temperature control unit of the tunnel provides a uniform temperature within an accuracy of $\pm 0.3^\circ\text{C}$. The schematics of the tunnel with the details of its sections is given in Figure 1. Section 7 of this figure has transparent glass walls of 5 m in length to allow the use of optical techniques. The experiments performed in this study was realized at 18 m downstream of the inlet of the wind tunnel test section. Detailed information about the LML wind tunnel is available in Carlier and Stanislas (2005).

Hot-wire Rake

Figure 2 shows the hot-wire rake of 143 single wire manufactured by LEA in order to provide both spatial and temporal information simultaneously. All the probes were distributed on an array in the plane normal to the flow (YZ plane) such that 11 probes were placed logarithmically in wall-normal direction on each vertical comb and 13 combs were staggered in spanwise direction. Figure 3 shows one of the combs at the wall. Each comb carried 9 single wire probes and one double probe with 2 single wire sensors. The double probe was used at the first position in the wall-normal direction on each comb due to limitations put by the spacing.

Each vertical comb was made of double-sided circuit printing board of 1.8 mm in thickness (Glaser, 1987, Delville, 1994, Delville et al., 1999). The high probe density around the center comb and close to the wall showed some evidence of blockage in the mean flow, but not in the turbulence quantities (when compared to measurements without the rake).

Special connectors as seen in Figure 4 were used between the combs and the 5 m long coaxial cables before connecting the probes to the anemometers. The connectors of the coaxial cables were isolated from each other to prevent any interference among each other.

The vertical combs in the spanwise direction were symmetrical about the center comb which was at $z=0$. The spanwise location of the vertical combs around the center comb were ± 4 mm, ± 12 mm, ± 28 mm, ± 60 mm, ± 100 mm and ± 140 mm. Diameter and length of the sensor wire of each probe were $2.5 \mu\text{m}$ and 0.5 mm, respectively. The probe

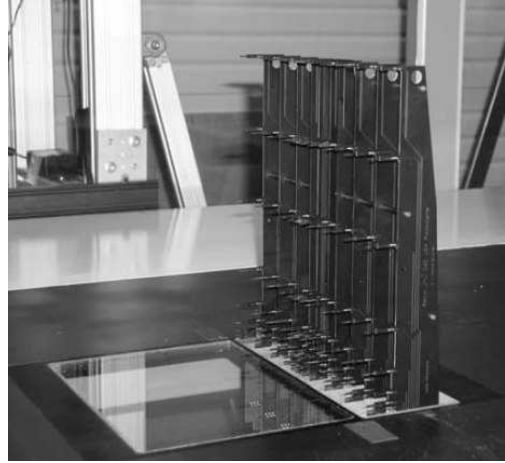


Figure 2: Hot-wire rake in place in the LML wind tunnel.



Figure 3: Close-up of one of the comb at the wall.

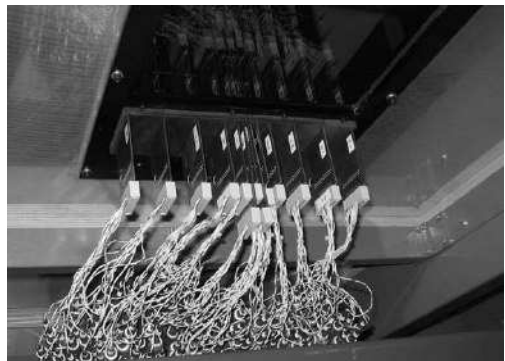


Figure 4: Connectors between the combs and the coaxial cables.

locations on each vertical comb in the wall-normal direction from wall toward freestream were 0.3 mm, 0.9 mm, 2.1 mm, 4.5 mm, 9.3 mm, 18.9 mm, 38.1 mm, 76.5 mm, 153.3 mm, 230.1 mm and 306.9 mm. The position of the first row of probes corresponded to y^+ of 3.75 and 7.5 for Re_θ of 9800 and 19100, respectively. The location of the last probe on each comb was at approximately δ_{99} . These coordinates

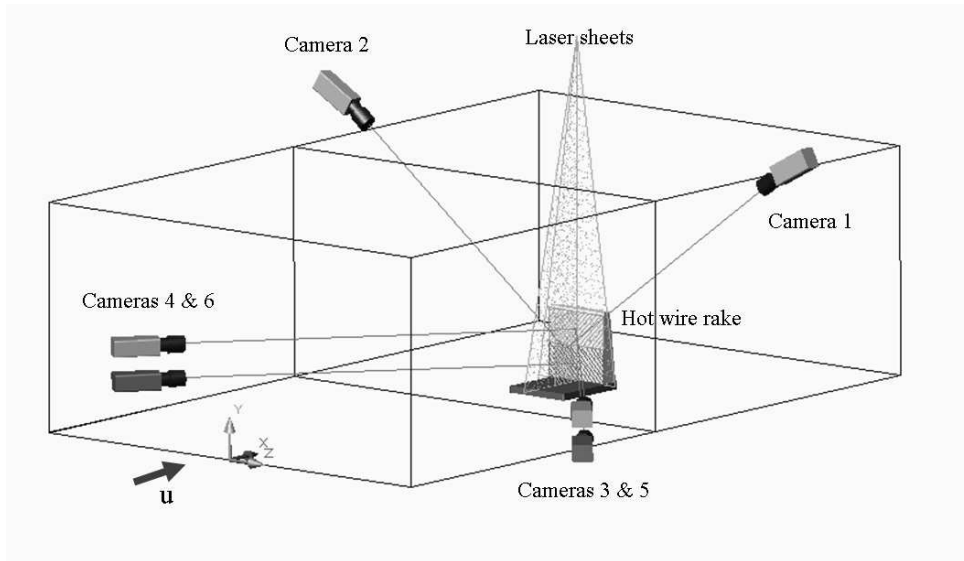


Figure 5: Setup 1: Synchronized 3 stereo PIV systems with HWR of 143 probes.

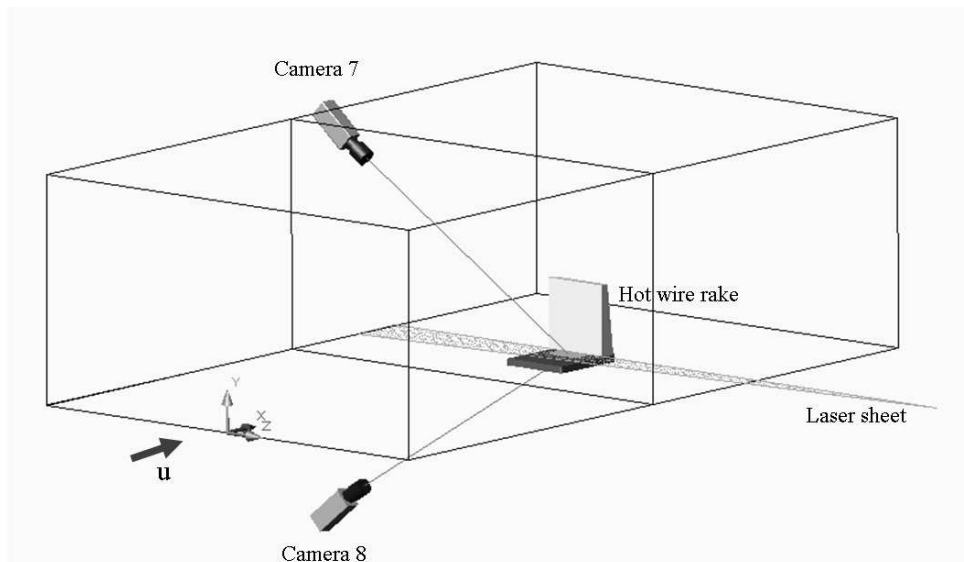


Figure 6: Setup 2: Synchronized high repetition stereo PIV system with HWR of 143 probes.

listed above were the design coordinates and there were imperfections at the probe locations particularly in wall-normal direction due to mechanical tolerances. The precise coordinate of each probe was computed by illuminating the tips of probes by a laser sheet and finding the relative position of each probe to the wall using the PIV cameras to record images. The deviations in positions of the probes from the design points were found to be less than ± 0.1 mm.

Hot-Wire Anemometers and Data Acquisition

A in-house developed 144 channel constant temperature hot-wire anemometer system with accompanying data acquisition system was set up and provided by the Turbulence Research Laboratory (TRL) of Chalmers University of Technology. The basic system was a modified version of that originally used by Citriniti et al. (2000) (see also Jung et al., 2004 and Gamard et al., 2004). Each anemometer was comprised of a Wheatstone bridge, output and sample/hold controls. (For details on the design, see Woodward, 2000

and Woodward et al., 2001.) A Microstar Laboratories DAP 5400a main board was used as the data acquisition board. This was an on-board operating system optimized for 32 bit operation in a PC expansion slot, consisting of an AMD K6-III + 400 MHz CPU with PCI bus interface, 14-bit A/D converter, with a 20 ns time resolution, 1.25M samples per second, and selective input/output range. The DAP 5400a was connected to the MSXB 029 analog backplane interface board, then to 3 analog input Microstar Laboratories expansion cards of type MSXB 018. The expansion cards were connected in series to each other via 68-line flat ribbon cables, and each one hold 4 connectors of 16 single-ended inputs. All channels were sampled simultaneously via sample/hold circuits on each anemometer and collected by DAP 5400a. Finally the data was saved to the physical disk of the computer. The hot-wire sampling frequency was set to 30 kHz for all channels at all different combinations. The data were sampled block-by-block and the length of sampling time of each block was 6 s.

Table 1: Synchronized HWR and PIV data collected during the experiments.

U_∞ (m s ⁻¹)	Re_θ	Configuration	Number of HWR blocks	Number of PIV records
10	19100	HWR + XY + YZ	600	9600
10	19100	HWR + XZ	1100	1100×40
10	19100	HWR + XZ	1 block of 2.29 s	6880 in 2.29 s
10	19100	HWR	613	0
			Total: 2314	
5	9800	HWR + XY + YZ	600	9600
5	9800	HWR + XZ	1100	1100×40
5	9800	HWR + XZ	1 block of 1.96 s	2943 in 1.96 s
5	9800	HWR	620	0
			Total: 2321	

The anemometers were stable, an especially important feature given the many hours of run time for a single experiment (typically 24 hours or more). Although the wind tunnel temperature and speed were held constant (to within $\pm 0.3^\circ\text{C}$. and less than 1% of freestream velocity respectively), the room temperature varied considerably throughout the day and night. There caused a slight thermal drift of the mean voltage which was less than most commercial units (see Johansson and George, 2006). Because of the very long data blocks it was possible to monitor and correct for this effect by using the statistics of the voltages for each block separately to adjust the calibration.

PIV Systems and Experimental Configurations

To be able to extract complete spatial and temporal information on the flow, two different combinations of synchronized PIV and HWR were set up. The first setup (shown in Figure 5) was comprised of three stereo PIV systems and the hot-wire rake. Two stereo PIV systems were used to record a YZ plane located 1 cm upstream of the hot-wire rake. Each of these two PIV systems covered a field of 30 cm in spanwise direction and 17 cm in wall-normal direction. The total area covered by the PIV systems was $30 \times 32 \text{ cm}^2$ with a small overlap between the two fields. The spatial resolution of both planes were 2 mm, meaning 20 and 40 wall units for Reynolds numbers of 9800 and 19100, respectively. These two systems used a BMI $2 \times 150 \text{ mJ}$ dual cavity Yag Laser and 4 Lavision Image Intense PIV cameras with a CCD of 1376×1024 pixels and a sampling rate of 4 velocity field per second (VF/s). A third stereo PIV system was to record a streamwise-wallnormal (XY) plane in the plane of symmetry ($z=0$). The dimensions of the plane were 10 cm in streamwise direction and 15 cm in wallnormal direction. Twice the spatial resolution for this plane was possible due to a decrease in size of the plane. This plane used a BMI $2 \times 150 \text{ mJ}$ dual cavity Yag Laser and 2 Lavision Flowmaster PIV cameras with a CCD of 1280×1024 and a sampling rate of 4 VF/s. Each PIV system recorded 16 samples during each block of hot-wire rake data.

In the second configuration as shown in Figure 6, one high repetition rate stereo PIV system synchronized with HWR was used in the streamwise-spanwise (XZ) plane to get both the spatial and temporal information in the near-wall region. The fields of view were $6.6 \times 3.4 \text{ cm}^2$ located at y^+ of 50 for the Reynolds numbers of 9800, and $4.2 \times 2.2 \text{ cm}^2$ at y^+ of 100 for the Reynolds number of 19100. The system was based on a Quantronix dual cavity $2 \times 20 \text{ mJ}$ YFL laser and two Vision Research Phantom V9 cameras of 1600×1200 pixels sizing $11.5 \times 11.5 \mu\text{m}^2$ each. Operational

number of pixels for the experiments were set to 384×592 pixels in the high Reynolds number case and 576×920 pixels in the low Reynolds number case. The sampling frequency of the high repetition PIV system was 3000 VF/s for the high Reynolds number experiment. The sampling frequency was then decreased to 1500 VF/s for the low Reynolds number case. In both cases 40 samples were recorded during each block of hot-wire rake data.

Seeding Particles

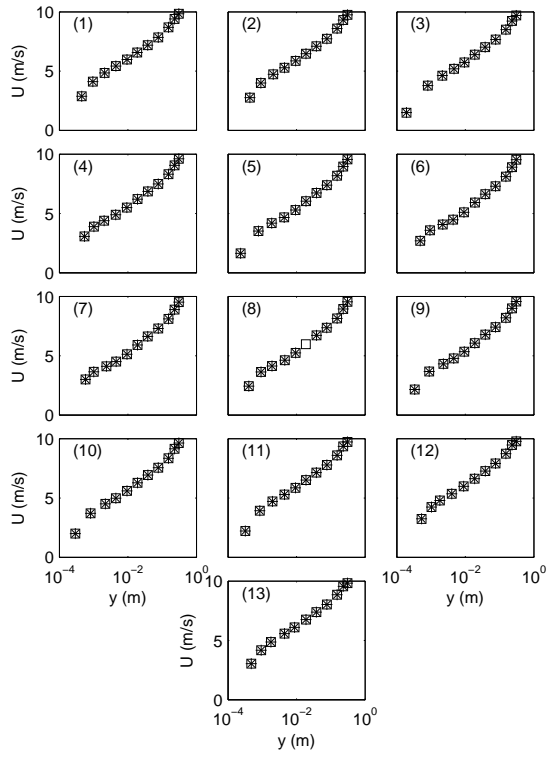
Poly-Ethylene Glycol was used as seeding fluid during the measurements. The size of the particles was of the order of $1 \mu\text{m}$. There was no evidence of contamination of the hot-wire sensors during the experiment, nor in the calibration constants, in agreement with the earlier experiments of Buchave (1979), Fronhpfel (2003) and Ewing et al. (2007). The synchronization of the PIV and HWR was made possible by means of an external clock. All systems were triggered by the external clock pulses and started reading data and images simultaneously. A PIV synchronization signal was recorded together with the HWR signals in order to get the time information.

Data Recorded

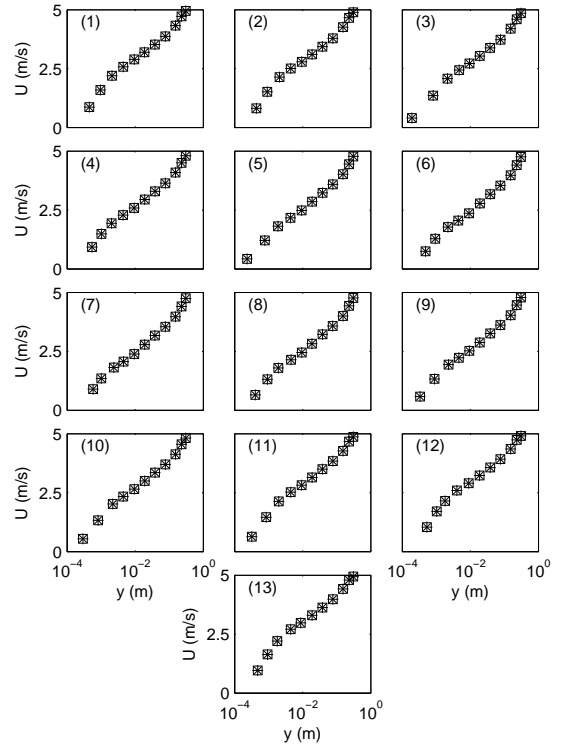
Table 1 summarizes the amount of data recorded during the experiments at the two different Reynolds number with the two different configurations of HWR and stereo PIV systems. For the first setup (Figure 5), 600 blocks of hot-wire data together with 600×16 velocity fields by the PIV were recorded for both Reynolds numbers. Following this case, 1100 blocks of hot-wire data were recorded with the second setup (e.g., Figure 6) simultaneously with 1100×40 velocity fields, provided by the high speed stereo PIV system. The same number of blocks of data was collected at both Reynolds numbers in this configuration. In the end one block of synchronized data was recorded by the high speed stereo PIV system with the full memory. This provided 6880 time resolved velocity fields of 2.29 s record length for the high Reynolds number case, and 2943 time resolved fields of 1.96 s record length for the low Reynolds number case. In addition, after completing the synchronized measurements, 613 and 620 blocks of hot-wire data were recorded alone for the high and low Reynolds numbers respectively.

PRELIMINARY RESULTS

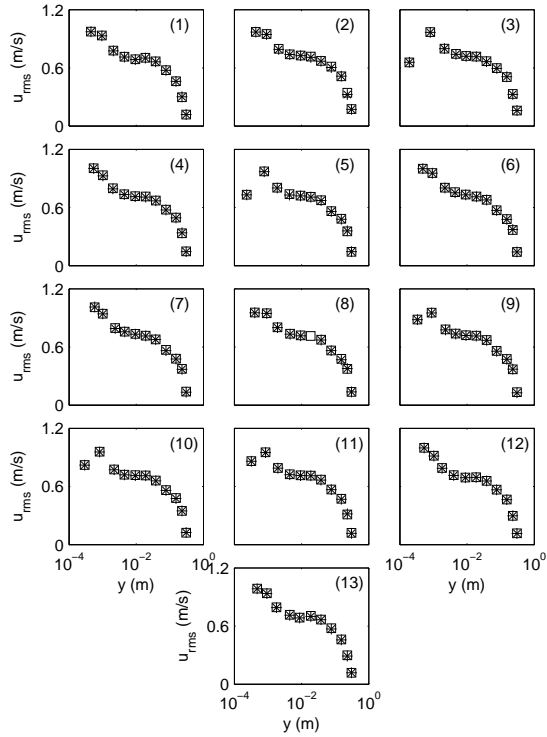
One of the biggest challenges in these experiments and the data reduction in the course of post-processing was to calibrate the hot-wire rake probes. Due to mechanical dif-



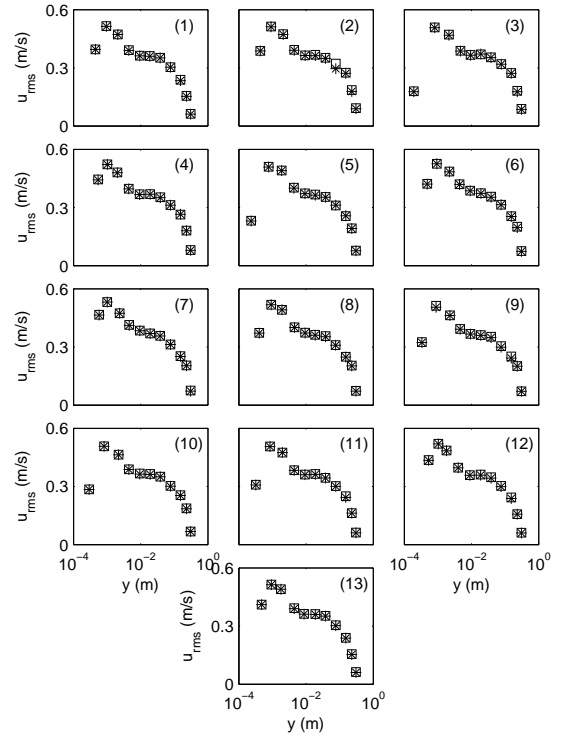
(a) Mean velocity profiles at $Re_\theta = 19100$.



(b) Mean velocity profiles at $Re_\theta = 9800$.



(c) RMS velocity profiles at $Re_\theta = 19100$.



(d) RMS velocity profiles at $Re_\theta = 9800$.

Figure 7: Velocity profiles from both PIV and HWR. Squares: PIV at HWR probe location, Stars: HWR. Inserted numbers within parenthesis represent the vertical comb numbers in a sequence. (1) is at $z = -140$ mm and (13) is at $z = 140$ mm.

difficulties and limited space in the wind tunnel, we had to perform the calibration of the hot-wire rake inside the turbulent boundary layer. Previously Breuer (1995) suggested a hot-wire calibration method in the turbulent flow field, which was essentially based on the functional (polynomial) relation between the mean velocities at the probe location and the statistics of the registered hot-wire voltages for corresponding mean velocities. The method itself is similar to the conventional polynomial calibration routines (George et al., 1989), but it includes some other higher order central moments of voltages, depending on the order of the polynomial function chosen. We initially implemented this proposed method for the hot-wire probe calibration, however we realized that the method only calibrates the mean velocity and not the fluctuating velocities. Therefore, a new calibration technique has been developed to take the velocity fluctuations into account, which is especially important in both highly turbulent regions and intermittent regions.

Calibration of the sensor in turbulence assumes the reference velocity to be known. These must either have been obtained in advance before putting hot-wire probes and/or rakes in place, or from a simultaneous and independent measurement (in this case the PIV) just upstream of the wires. The former assumes there to be no blockage effects because of the existence of the rake. Since the blockage creates a potential flow disturbance while the turbulence/mean flow interaction occurs over some distance, the effect shows itself in the mean velocity distribution. By using PIV and HWR simultaneously, it was possible to detect that there was indeed some blockage effect around the centerline and near the wall, consistent with the higher probe density here. Moreover it was possible to verify that the blockage did not affect the second and higher order turbulence moments, as expected. Therefore, we performed the final calibration by using the PIV data simultaneously taken together with the hot-wire rake signals (e.g., Figure 5).

Figure 7 shows the initial results from both the PIV and HWR. The mean streamwise velocity profiles and profiles of root mean squares of the streamwise velocity fluctuation are given for both Reynolds numbers. As it is seen in these figures, there is near perfect agreement between the PIV and HWR results. We have also observed the same level of agreement in both third and fourth central moments of streamwise velocity.

The data reduction is still in process, and will continue for some time. This will include all possible two-point spatial and temporal cross-spectra between the hot-wire and PIV locations. Updates about the data will be available through the WALLTURB research project official web page (<http://wallturb.univ-lille1.fr/>).

ACKNOWLEDGEMENTS

This work has been performed under the WALLTURB project. WALLTURB (A European synergy for the assessment of wall turbulence) is funded by the CEC under the 6th framework program (CONTRACT No: AST4-CT-2005-516008).

REFERENCES

Breuer, K. S., 1995, "Stochastic Calibration of Sensors in Turbulent-Flow Fields," *Experiments in Fluids*, Vol. 19, No. 2, pp. 138-141.

Buchave, P., 1979, "The Measurement of Turbulence

with the Burst-Type Laser Doppler Anemometer - Errors and Correction Methods," Ph.D. Thesis, State University of New York at Buffalo, Buffalo, NY, USA.

Carlier, J., and Stanislas, M., 2005, "Experimental Study of Eddy Structures in a Turbulent Boundary Layer Using Particle Image Velocimetry," *Journal of Fluid Mechanics*, Vol. 535, pp. 143-188.

Citriniti, J. H., and George W. K., 2000, "Reconstruction of the Global Velocity Field in the Axisymmetric Mixing Layer Utilizing the Proper Orthogonal Decomposition," *Journal of Fluid Mechanics*, Vol. 418, pp. 137-166.

Delville, J., 1994, "Characterization of the Organization in Shear Layers via the Proper Orthogonal Decomposition," *Applied Scientific Research*, Vol. 53, Nos. 3-4, pp. 263-281.

Delville, J., Ukeiley, L., Cordier, L., Bonnet, J. P., and Glauser, M., 1999, "Examination of Large-Scale Structures in a Turbulent Plane Mixing Layer. Part 1. Proper Orthogonal Decomposition," *Journal of Fluid Mechanics*, Vol. 391, pp. 91-122.

Ewing, D., Frohnapfel, B., George, W. K., Pedersen, J. M., and Westerweel, J., 2007, "Two-Point Similarity in the Round Jet," *Journal of Fluid Mechanics*, Vol. 577, pp. 309-330.

Foucaut, J. M., Carlier, J., and Stanislas, M., 2004, "PIV Optimization for the Study of Turbulent Flow Using Spectral Analysis," *Measurement Science and Technology*, Vol. 15, No. 6, pp. 1046-1058.

Frohnapfel, B., 2003, "Multi-Point Similarity of the Axisymmetric Turbulent Far Jet and Its Implication for the POD," M.Sc. Thesis, Chalmers University of Technology/Friedrich-Alexander-Universität at Erlangen-Nürnberg, Gothenburg, Sweden and Erlangen, Germany.

Gamard, S., Jung, D. H., and George, W. K., 2004, "Downstream Evolution of the Most Energetic Modes in a Turbulent Axisymmetric Jet at High Reynolds Number. Part 2. The Far-Field Region," *Journal of Fluid Mechanics*, Vol. 514, pp. 205-230.

George, W. K., Beuther, P. D., and Shabbir, A., 1989, "Polynomial Calibrations for Hot Wires in Thermally Varying Flows," *Experimental Thermal and Fluid Science*, Vol. 2, No. 2, pp. 230-235.

Glauser, M. N., 1987, "Coherent Structures in the Axisymmetric Turbulent Jet Mixing Layer," Ph.D. Thesis, State University of New York at Buffalo, Buffalo, NY, USA.

Johansson, P. B. V., and George, W. K., 2006, "The Far Downstream Evolution of the High Reynolds Number Axisymmetric Wake Behind a Disk. Part 1. Single Point Statistics," *Journal of Fluid Mechanics*, Vol. 555, pp. 363-385.

Jung, D. H., Gamard, S., and George, W. K., 2004, "Downstream Evolution of the Most Energetic Modes in a Turbulent Axisymmetric Jet at High Reynolds Number. Part 1. The Near-Field Region," *Journal of Fluid Mechanics*, Vol. 514, pp. 173-204.

Woodward, S. H., 2001, "Progress Toward Massively Parallel Thermal Anemometry System," M.Sc. Thesis, State University of New York at Buffalo, NY, USA.

Woodward, S. H., Ewing, D., and Jernqvist, L., 2001, "Anemometer System Review," *ASME Sixth International Thermal Anemometry Symposium*, Melbourne, Australia.